Electronic Supplementary Material (ESI) for ChemComm.

High-conductivity Thiocyanate Ionic Liquid Interface Engineering for Efficient and stable Perovskite Solar Cell

Shumao Wang, ‡[a], Haodan Guo, ‡[b,c] Jinpeng Wu, [b,c] Yan Lei, [b,c] Xiangrong Li, [b,c] Yanyan Fang, *[b,c] Yuhua Dai *[a], Wanchun Xiang*[d] and Yuan Lin*[b,c]

a. College of New Materials and Chemical Engineering, Beijing Institute of Petrochemical Technology, Beijing 102617, China. e-mail: daiyuhua@bipt.edu.cn.

b. Beijing National Laboratory for Molecular Sciences, CAS Research / Education Center for Excellence in Molecular Sciences, Institute of Chemistry, Chinese Academy of Science, Beijing 100190, China. e-mail: fyy001@iccas.ac.cn, linyuan@iccas.ac.cn.

c. University of Chinese Academy of Sciences, Beijing 100049, China

d. Key Laboratory of Applied Surface and Colloid Chemistry, Ministry of Education, Shaanxi Key Laboratory for Advanced Energy Devices, Shaanxi Engineering Lab for Advanced Energy Technology, School of Materials Science and Engineering, Shaanxi Normal University, Xi'an, 710119, China. e-mail: wanchun.xiang@snnu.edu.cn.

‡These authors contributed equally to this work

Experimental Section

Materials: SnO_2 colloid precursor (tin (iv) oxide, 15% in H_2O colloidal dispersion) was purchased from Alfa Aesar. Lead iodide (PbI_2, ≥99.99%), formamidinium iodide (FAI, ≥99.9%), methylammonium iodide (MAI, ≥99.9%), methylammonium chloride (MACl, ≥99.9%) and bis(trifluoromethane) sulfonimide lithium salt (Li-TFSI, ≥99.8%) were all bought from Xi'an Polymer Light Technology in China. Dimethylformamide (DMF), dimethyl sulfoxide (DMSO), isopropanol (IPA), chlorobenzene (CB) and acetonitrile were all purchased from Sigma-Aldrich. 2,2',7,7'-tetrakis ITO glass and (N, N-p-dimethoxyphenylamino)-9,9'-spirobifluorene (Spiro-OMeTAD, ≥99.9%) was purchased from Liaoning Youxuan New Energy Technology Co., Ltd. 1-Ethyl-3-methylimidazolium thiocyanate (EMIMSCN, ≥ 98%) was purchased from TCI. All materials were used without further purification.

Device fabrication: The ITO glass was cleaned sequentially by deionized water, acetone, ethanol, and IPA in an ultrasonic bath for 20 min, respectively. Before the deposition electron transport layer, the substrates were dried by high-purity nitrogen and then exposed to ultraviolet ozone for 20 min. Then SnO_2 nanoparticle solution with 2% in water was spin-coated onto the ITO glass at 4000 rpm for 30 s, and annealed at 180 °C for 30 min under ambient air. The ITO/SnO_2 substrates were treated with ultraviolet ozone for 20 min to improve the surface wettability. PbI_2 solution (691.5 mg/mL in DMF/DMSO mixed solvent (9:1)) was spin-coated onto SnO_2 at 1500 rpm for 30 s and annealed at 70°C for 1 min in an inert gas atmosphere. Next, a mixture solution of FAI:MAI:MACl was spin-coated onto the PbI_2 layers at rate 2000 rpm for 30 s, followed by annealing at 150°C for 15 min in ambient air conditions (30-40% humidity). For EMIMSCN treatment, the EMIMSCN/IPA solution was deposited by spin-coating at 5000 rpm for 30 s onto the perovskite surface, respectively. 28.8 μL 4-tertbutylpyridine (tBP) and 17.5 μL LiTFSI solution (520 mg LiTFSI in 1 ml acetonitrile) were added into the Spiro-OMeTAD solution (72.3 mg in 1mL) to prepared the hole transport layer at a spin rate of 3000 rpm for 30 s. Finally, 10 nm of MoO_3 film as buffer layer and Ag as electrode was thermally evaporated on it under a pressure of 5×10^{-5} Torr. The shadow mask areas are 0.06 cm^2.

Measurements and Characterization

The photovoltaic performance of PSCs was carried out under one sun illumination (AM 1.5, 100 mW cm^{-2}) by Keithley 2400 digital source meter. The light intensity was calibrated by a silicon reference cell with KG1 filter (Enli tech. Co. Ltd, Taiwan). The reverse scan ranged from 1.20 V to -0.02 V with a scan rate of 10 mV and 10 ms delay time, while the forward scan ranged from -0.02 V to 1.20 V. External quantum efficiency (EQE) spectra of the devices were measured by a Solar Cell Spectral Response Measurement System QE-R3-011 (Enli Technology Co. Ltd., Taiwan). The X-ray photoelectron spectroscopy (XPS) analysis were conducted by ESCALA250XI XPS equipment (Thermo Fisher Scientific) and Al Kα X-ray radiation as the X-ray source to generate the photoelectrons. A non-monochromated He I photon source (hv = 21.22 eV) was used as ultraviolet radiation source on a photoelectron spectrometer (ESCALAB250XI) for the ultraviolet photoelectron spectroscopy (UPS) measurements. The scanning electron microscope (SEM) was performed on the field-emission scanning electron microscopy (Hitachi S-4800) under an accelerated voltage of 10 kV. The atomic force microscopy (AFM) and scanning Kelvin probe microscopy (SKPM) characterizations were obtained by MFP-3D AFM (Asylum Research, Oxford Instruments). The steady-state photoluminescence (PL) spectrum was tested by FluoroMax+ spectrometer. The time-resolved photoluminescence (TRPL) spectrum was collected by FLS980 spectrometer. X-ray diffraction (XRD) patterns were investigated by D/max 2500 with Cu kα1 radiation with a scan rate of 8 ° min^{-1}. The absorbance spectrum of perovskite film was collected by ultraviolet-visible (UV-Vis) spectrometer (HITACHI U3010).

DFT calculation

Density functional theory (DFT) calculations were carried out using Dmol3 code.[1] The exchange and correlation energies were determined with the Perdew, Burke, and Ernzerhof (PBE) functional within the generalized gradient approximation (GGA).[2] The DFT semi-core pseudo potentials (DSPP) core treatment is implemented for relativistic effects, which replaces core electrons by a single effective potential and introduces some degree of relativistic correction into the core. Moreover, the double numerical plus polarization (DNP) is chosen as the basis set.[3] Among the basis sets provided by $dmol^3$ code, the DNP basis set has the best accuracy and highest computational cost. A thermal smearing of 0.005 Ha (1 Ha = 27.21 eV) to the orbital occupation is applied to speed up electronic convergence. The convergence tolerance of electronic structure and geometry optimization are 1×10^{-5} Ha, 2×10^{-3} Ha/Å, respectively. The global orbital cutoff is 5.0 Å. In the electrostatic potential calculations, the grid interval and boundary were set to 0.1 Å and 3.0 Å, respectively. The 2×2 supercell of $FAPbI_3$ (010) was used to build the calculation models. The atoms in the bottom 3 layers were fixed, and the other atoms were fully relaxed. In the $FAPbI_3$ (010) model, I atom on one surface was removed to build the V_I calculation model, and one extra I atom was replaced with Pb atom to build the Pb_I calculation model. A vacuum height of 20 Å along the vertical direction was selected to avoid the unwanted interaction between the slab and its period images. The optimized molecules obtained from the cluster model were placed in the corresponding defect sites as the initial configuration of the adsorption structure. Through geometric optimization calculation of the initial configuration, the stable adsorption configuration and binding energy (Eb) were obtained. The binding energy (E_b) of adsorbate on surface are calculated through,

$$\boldsymbol{Eb(M) = E_{SVS} - E_M - E_S}$$

where E_{sys}, E_M, and E_s are the DFT calculated energies of the adsorption systems, an isolated ion with corresponding charge, and surface, respectively.

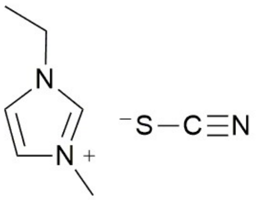

Scheme S1. The structure of 1-Ethyl-3-methylimidazolium thiocyanate (EMIMSCN)

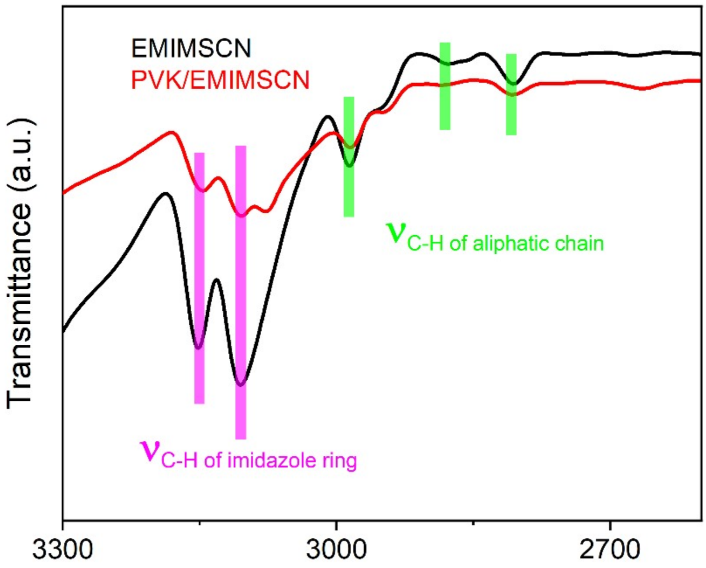

Figure S1. FTIR spectra of the control and EMIMSCN-treated perovskite films (PVK/EMIMSCN).

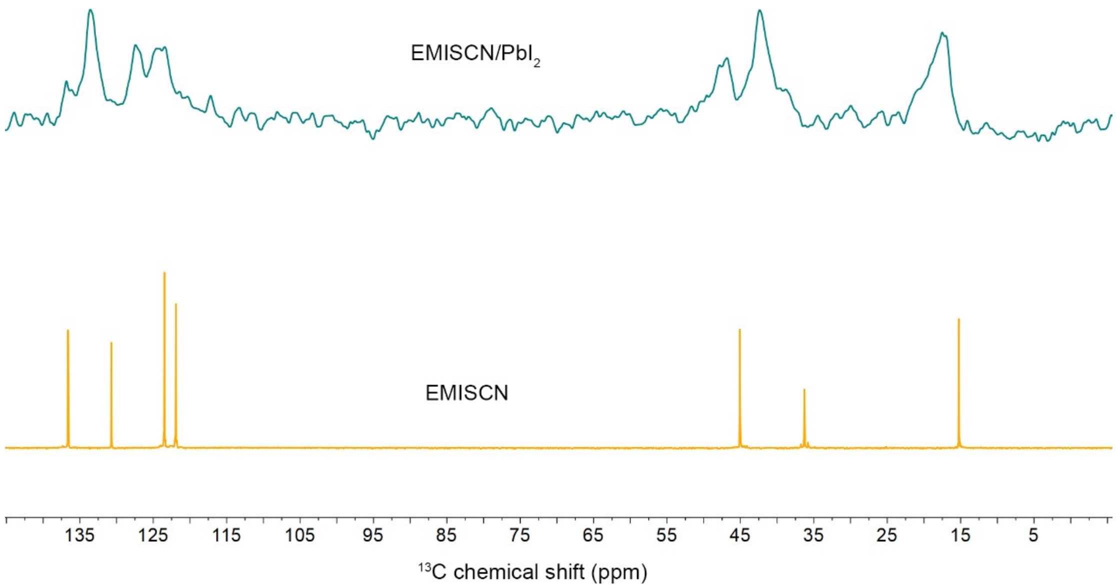

Figure S2. ^{13}C NMR spectra of EMIMSCN and EMIMSCN/PbI_2

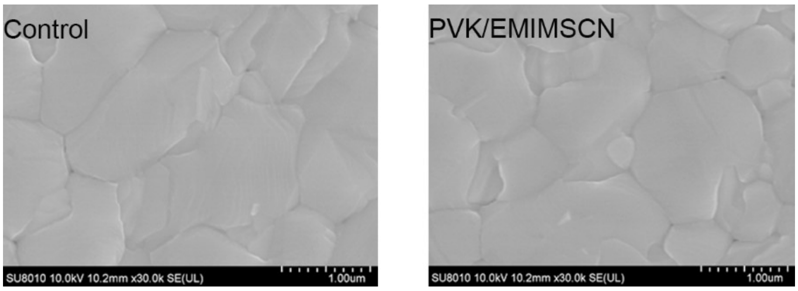

Figure S3. Top-view SEM images of control and PVK/EMIMSCN film.

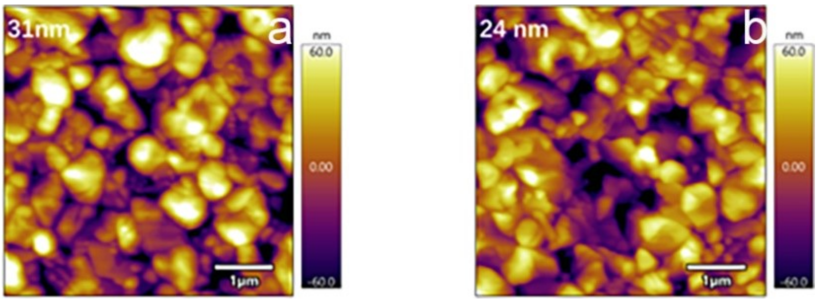

Figure S4. AFM images of control and PVK/EMIMSCN film.

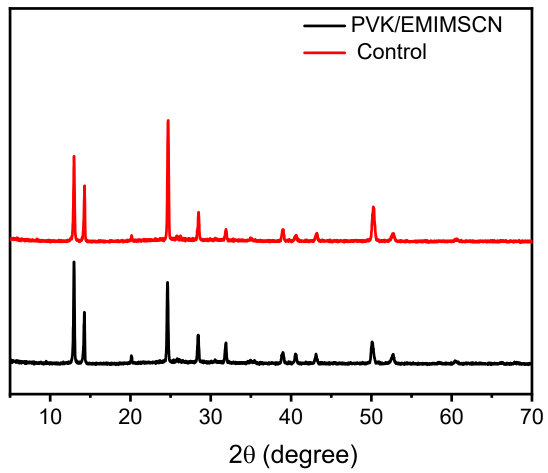

Figure S5. X-ray diffraction (XRD) of control and PVK/EMIMSCN film.

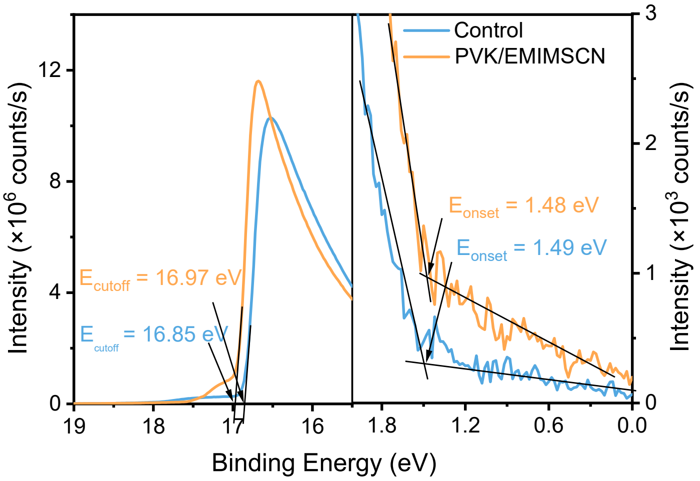

Figure S6. Ultraviolet photoelectron emission spectra (UPS) of control and PVK/EMIMSCN film.

The work function (WF), VB (the energy value of valence band maximum) and CB (the energy value of conduction band minimum) values based on UPS measurements were calculated by the following equations:

$$WF = h\upsilon - E_{cutoff} \qquad \text{(S1)}$$

$$VB = -(WF + E_{onset}) \qquad \text{(S2)}$$

$$CB = VB + E_g \qquad \text{(S3)}$$

where hv is photon energy (21.22 eV), E_{cutoff} is the cutoff energy, E_{onset} is the onset energy, and E_g is the energy bandgap. Figure S6 exhibit full spectra, cutoff regions and onset regions of pristine perovskite and EMIMSCN-treated perovskite films, respectively. From the UV-VIS absorbance of the pristine perovskite and EMIMSCN-treated perovskite, the E_g almost remained the same, with a value of 1.55 eV.

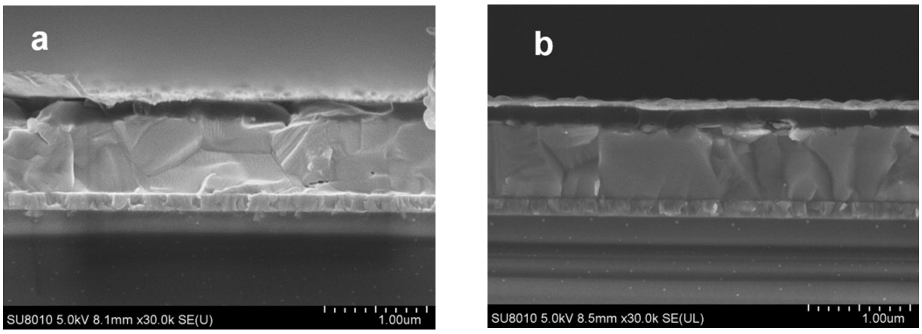

Figure S7. The cross-sectional SEM images of PSCs devices.

Table S1. Kinetic parameters extracted from the TRPL spectrum without ETL.

Devices	τ_1 [ns]	B_1 [%]	τ_2 [ns]	B_2 [%]	τ_{ave} [μs]
Quartz/Perovskite	514.01	804.16	1228.26	330.49	0.80
Quartz/Perovskite/EMIMSCN	327.74	149.34	1625.91	476.63	1.60

TRPL decay can be fitted with the biexponential equation (Equation (1)) and the fitting parameters are listed in Table S1.

$$f(t) = C + B_1 \exp\left(\frac{-t}{\tau_1}\right) + B_2 \exp\left(\frac{-t}{\tau_2}\right) \quad \text{Equation (1)}$$

$$\tau_{ave} = \frac{B_1\tau_1^2 + B_2\tau_2^2}{B_1\tau_1 + B_2\tau_2} \quad \text{Equation (2)}$$

where C is a constant, B_1 and B_2 are the relative amplitudes, τ_1 is the carrier lifetime for the fast component recombination and τ_2 is the carrier lifetime for the slow component recombination. The average carrier lifetime is estimated by Equation (2).[4]

Table S2. The detailed photovoltaic parameters of PSCs with and without EMIMSCN

Devices	Direction	V_{oc} / V	J_{sc} / mA cm^{-2}	FF / %	PCE / %	HI / %
PVK/EMIMSCN	Reverse	1.15	25.69	77.75	22.55	5.60
	Forward	1.14	25.01	74.90	21.28	
Control	Reverse	1.10	24.78	73.46	20.11	10.5
	Forward	1.07	24.42	68.36	18.00	

References

1. B. Delley, *J. Chem. Phys.*, 2000, **113**, 7756-7764.
2. J. P. Perdew, K. Burke and M. Ernzerhof, *Phys. Rev. Lett*, 1996, **77**, 3865-3868.
3. B. Delley, *J. Chem. Phys.*, 1990, **92**, 508-517.
4. F. Li, X. Deng, F. Qi, Z. Li, D. Liu, D. Shen, M. Qin, S. Wu, F. Lin, S.-H. Jang, J. Zhang, X. Lu, D. Lei, C.-S. Lee, Z. Zhu and A. K. Y. Jen, *J. Am. Chem. Soc.*, 2020, **142**, 20134-20142.